Energetic and Economic Analysis of a Solar Assisted Heat Pump for Pasteurization Process

Giampaolo Manzolini[1], Michele Merlo[1], Luca Molinaroli[1], Riccardo Simonetti[1]

[1] Dipartimento di Energia, Politecnico di Milano, Milano (Italy)

Abstract

In the present paper, the energetic and economic analysis of a solar-assisted heat pump for an industrial pasteurization process is investigated. The considered system consists of thermal energy storage, a water-to-water heat pump and a solar field made up of both photovoltaic-thermal collectors and evacuated tube collectors. A mathematical model of each component of the system is built and validated, while the overall model of the system is built with a bottom-up approach. The energetic and economic analysis is performed on a yearly basis varying the storage size and the solar field size and considering a boiler-only scenario as the reference system. The results show that, from the energetic point of view, the best system could provide up to 90% of the energy required by the process and, consequently, significantly reduce auxiliary boiler consumption. On the other side, from an economic point of view, the best solution provides a minimum payback time approximately equal to 8 years with 14.4% internal rate of return.

Keywords: Economic analysis, Energetic analysis, Pasteurization, Solar assisted heat pump

1. Introduction

According to Eurostat (Eurostat, 2021), in 2019 the industrial sector is responsible of 25.6% of final energy consumption in Europe. Five sectors, i.e. chemical, non-metallic minerals, paper, food and steel industries, accounts for about two thirds of the total energy consumption in industry (Papapetrou et al., 2018) and both heat and electricity are energy carriers. Electricity is widely used in motors, compressors and lightning, while the process heat is required in a wide range of temperatures, starting from about 100 °C in food and textiles industries to more than 500 °C in metal processing industries.

Among the industrial process in the food industry, the pasteurization process is considered a low temperature process since it requires heat at temperature in the range 65 °C – 120 °C (Brückner et al., 2015). Although this low-mid temperature heat is typically supplied by a boiler, an improvement of the overall pasteurization process energetic performance could be achieved considering heat pumps. Indeed, a lot of research efforts are currently being put in mid-high temperature heat pump development (Arpagaus et al., 2018, Van de Bor et al., 2013) due to the superior energetic and environmental performance of this technology.

An even more interesting alternative to the conventional boiler could be the solar assisted heat pump (SAHP) system that relies upon the integration of a solar field with a heat pump in which the hot water at solar field outlet is used as cold heat source in the heat pump evaporator. In this way it is possible to exploit solar radiation more efficiently, since the water temperature may be significantly lower than the temperature required by the process, improving both the heat pump and the solar collector efficiencies. In the open literature, a lot of experimental or numerical analyses SAHP systems are carried out demonstrating the superior performance of this integrated system with respect to traditional systems such as boiler or conventional heat pump (Kamel et al., 2015, Mohanraj et al. 2018, Lazzarin, 2020, Simonetti et al. 2019, 2020). However, all the available studies deal with SAHP systems at residential scale and there is lack of analysis of their application to industrial processes.

Therefore, in the present work an energetic and economic analysis of the use of mid temperature SAHP system in a pasteurization process is carried out with the aim of demonstrating its feasibility in an industrial scenario.

doi:10.18086/swc.2021.29.06 Available at http://proceedings.ises.org

2. System modelling

The system under investigation is a solar assisted heat pump system used to supply heat to a pasteurization process. The layout of the system is shown in Fig. 1 and, besides the pasteurization process itself, it consists of:

- A heat pump that supplies heat to the pasteurization process.
- A solar field where both photovoltaic/thermal collectors (PV/T) and evacuated tube collectors (ETC) are considered. The PV/Ts are used to produce low temperature heat which, in turn, is used as cold heat source in the heat pump evaporator whereas the hot water at ETCs may be exploited either in the heat pump evaporator or in the pasteurization process depending on its temperature.
- A heat storage which stores the system excess heat allowing for larger solar source exploitation.
- An auxiliary boiler that is used only when the SAHP system, together with the heat storage, cannot provide the heat required by the pasteurization process (low solar radiation and/or low amount of heat in the storage). The auxiliary boiler is aimed to allow continuous system operation during the whole year.

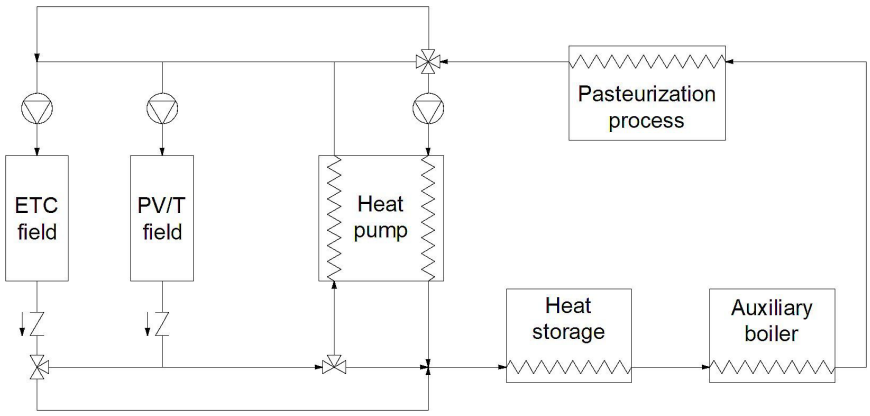

Fig. 1: Layout of the solar assisted heat pump system for pasteurization process

The model of the system is built starting from the model of each component as detailed in the next sections.

2.1 Heat pump

The heat pump considered in this work is a water-to-water heat pump system working with carbon dioxide in transcritical mode. The refrigerant properties are calculated using Refprop 9.1 (Lemmon et al., 2013) whereas the layout of the heat pump is shown in Fig. 2.

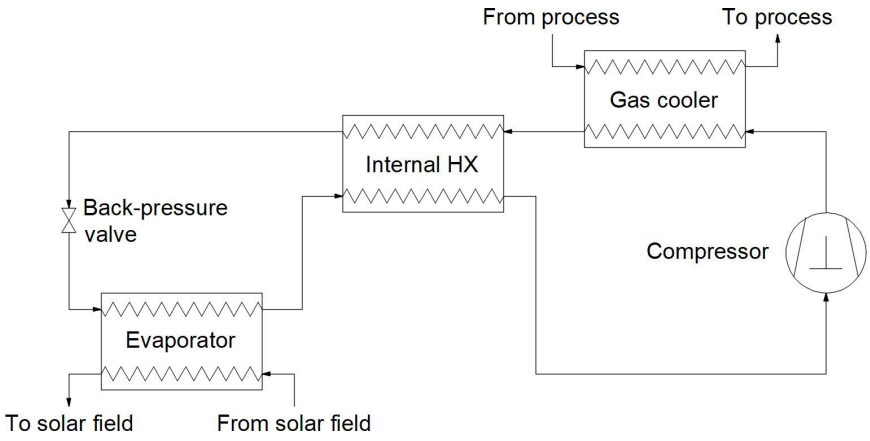

Fig. 2: Layout of the heat pump

The model of the heat pump is a steady-state model built with a bottom-up approach. The model of each component of the heat pump is first realized and then the overall heat pump model is built assembling them together.

The compressor considered in the present work is a variable speed reciprocating compressor. The compressor is modelled using the polynomial functional form provided by the manufacturer that allows for the calculation of

refrigerant mass flow rate or compressor power as a function of evaporating temperature and gas cooler outlet pressure:

$$\dot{m} = a_1 + a_2 T_E + a_3 p_{O,GC} + a_4 T_E^2 + a_5 T_E p_{O,GC} + a_6 p_{O,GC}^2 + a_7 T_E^3 + a_8 T_E^2 p_{O,GC} + a_9 T_E p_{O,GC}^2 + a_{10} p_{O,GC}^3 \quad \text{(eq. 1)}$$

$$\dot{W} = b_1 + b_2 T_E + b_3 p_{O,GC} + b_4 T_E^2 + b_5 T_E p_{O,GC} + b_6 p_{O,GC}^2 + b_7 T_E^3 + b_8 T_E^2 p_{O,GC} + b_9 T_E p_{O,GC}^2 + b_{10} p_{O,GC}^3 \quad \text{(eq. 2)}$$

The 10 coefficients that appear in Eqs. (1-2) depend on the rotational frequency of the compressor shaft and are taken from the manufacturer's datasheet. Since the model is valid only for a refrigerant superheating at compressor suction equal to 10 K, the corrective action proposed by Dabiri and Rice (1981) is used to account for a different superheat. Finally, due to the heat pump application, the compressor is assumed to be adiabatic and, therefore, the following equation applies for the calculation of refrigerant enthalpy at compressor discharge:

$$h_{\mathrm{DIS}} = h_{\mathrm{SUC}} + \dot{W}/\dot{m} \quad \text{(eq. 3)}$$

The three heat exchangers are modelled using a finite volume approach. Each heat exchanger is divided in small slices and the amount of heat transferred between the hot and cold fluid in the small volume is calculated using the ε-NTU method according to the following equations:

$$\varepsilon = \frac{\dot{Q}}{\dot{Q}_{MAX}} = \frac{1-exp[-NTU(1-R^*)]}{1-R^* exp[-NTU(1-R^*)]} \quad \text{(eq. 4)}$$

$$\dot{Q} = \dot{m}_H c_{P,H}\left(T_{H,IN} - T_{H,OUT}\right) = \dot{m}_C c_{P,C}\left(T_{C,OUT} - T_{C,IN}\right) \quad \text{(eq. 5)}$$

$$\dot{Q}_{MAX} = \min\left(\dot{m}_H c_{P,H}, \dot{m}_C c_{P,C}\right)\left(T_{H,IN} - T_{C,IN}\right) \quad \text{(eq. 6)}$$

$$R^* = \frac{\min\left(\dot{m}_H c_{P,H}, \dot{m}_C c_{P,C}\right)\left(T_{H,IN} - T_{C,IN}\right)}{\max\left(\dot{m}_H c_{P,H}, \dot{m}_C c_{P,C}\right)\left(T_{H,IN} - T_{C,IN}\right)} \quad \text{(eq. 7)}$$

$$NTU = \frac{\mathrm{UA}}{\min\left(\dot{m}_H c_{P,H}, \dot{m}_C c_{P,C}\right)\left(T_{H,IN} - T_{C,IN}\right)} \quad \text{(eq. 8)}$$

$$(UA)^{-1} = \left(h_{\mathrm{C,H}} A\right)^{-1} + t_W (k_{\mathrm{W}} A)^{-1} + \left(h_{\mathrm{C,C}} A\right)^{-1} \quad \text{(eq. 9)}$$

The overall heat transfer rate is, then, the sum of the infinitesimal heat transfer rate at volume scale.

The correlation used for the calculation of the heat transfer coefficient are an in-house correlation for the single phase fluid (water in evaporator and gas cooler, carbon dioxide in gas cooler, internal heat exchanger and vapour zone in evaporator) whereas the correlation proposed by Longo et al. (2015) is used in the two-phase zone of the evaporator.

Finally, the back-pressure expansion valve is modelled considering an isenthalpic process and assuming that the valve is able to keep the gas cooler outlet pressure at the optimal value in any heat pump operating conditions.

2.2 Solar collectors

As stated, the solar collectors used in the present study are both photovoltaic/thermal collectors (PV/T) and evacuated tube collectors (ETC). For the sake of simplicity, and similarly to the heat pump model, the soalr collector models are steady-state too.

Considering the PV/Ts first, both an electrical model and a thermal model is needed. The electrical model used in the present work computes the electrical efficiency with the power coefficient approach (Zondag et al., 2003) assuming, for the sake of simplicity, that the PV cell temperature is 10 °C higher than the water average temperature:

$$\eta_{EL} = \eta_{EL,REF}\left[1 + \gamma_{PVT}\left(\bar{T}_W + 10 - T_{CELL,REF}\right)\right] \quad \text{(eq. 10)}$$

whereas the thermal model computes the thermal efficiency as a function of optical efficiency and thermal losses which, in turn, depends on the reduced temperature. Due to the low operating temperature of this collector, only the linear term is considered and, similarly to the electrical model, the water average temperature is used for the sake of simplicity:

$$\eta_{TH} = \eta_{OPT} - k_{1,PVT}\frac{(\bar{T}_W - T_A)}{G} \quad \text{(eq. 11)}$$

ETC collectors need only a thermal model which is very similar to that of PV/Ts. Indeed, again, the thermal model of ETC computes the thermal efficiency as a function of optical efficiency and thermal losses but the quadratic term is considered for this type of collector due to the higher operating temperatures:

$$\eta_{TH} = \eta_{OPT} - k_{1,ETC}\frac{(\bar{T}_W - T_A)}{G} - k_{2,ETC}\frac{(\bar{T}_W - T_A)^2}{G} \quad \text{(eq. 12)}$$

The constants that appear in eqs. (10-12) are taken from manufacturers' datasheets.

2.3 Heat storage, boiler and pumps

Finally, simple models are developed also for the heat storage, the auxiliary boiler and the pumps.

The heat storage is modelled as a perfectly stratified heat storage where the thermocline is adiabatic and has a thickness equal to zero. No mixing phenomena occur when water is injected to or extracted from it. The storage is assumed to be well insulated, therefore the heat loss to the environment is neglected.

The boiler is modelled as a constant efficiency thermal system. The boiler efficiency is chosen averaging the value reported in several manufacturers' datasheet.

Pumps are modelled in order to account for the pumping power in the overall system consumption. First, pressure drop in the evaporator or in the solar collectors is calculated using the following equation:

$$\Delta p = c_1 + c_2\dot{v}_W + c_3\dot{v}_W^2 \quad \text{(eq. 13)}$$

The constants that appear in eq. 13 are taken from manufacturers' datasheet (solar collectors) or are regressed using a best fitting procedure over manufacturer's performance data (brazed plate evaporator).

Once the pressure drop is calculated, the pumping power is computed according to eq. 14 in which the pump efficiency is taken from manufacturers' datasheet:

$$\dot{W}_{PUMP} = \frac{\dot{v}_W \Delta p}{\eta_{PUMP}} \quad \text{(eq. 14)}$$

3. Case study

As stated, the goal of the present study is to assess the energetic and economic performance of a SAHP for pasteurization process. With the aim of making the analysis as simple as possible, without loosing accuracy or consistency with a real pasteurization process, the pasteurization process is assumed to operate continuously, i.e. 24 hours a day and 7 days a week. Additionally, it is assumed that a water mass flow rate equal to $\dot{m}_W = 1\ \mathrm{kg \cdot s^{-1}}$ at $T_{W,IN} = 80$ °C and $T_{W,OUT} = 50$ °C may fulfill both the temperature requirements and the process heating load.

In order to improve the feasibility of the SAHP system, only commercially available components are chosen. The characteristics of the main components of the system studied are collected in Tab. 1.

Tab. 1: Main characteristics of the components of the SAHP system

Component	Parameter and value
Compressor	Variable speed reciprocating compressor, swept volume 30.75 $m^3 \cdot s^{-1}$, rotational frequency 30 Hz – 70 Hz
Gas cooler	329 mm x 119 mm, 138 plates, heat transfer area 5.58 m^2
Evaporator	329 mm x 119 mm, 92 plates, heat transfer area 3.68 m^2
Internal HX	329 mm x 119 mm, 72 plates, heat transfer area 2.88 m^2

PV/T	Area 1.63 m^2, $\eta_{OPT} = 0.528$, $k_{1,PVT} = 13.658$ W·m^{-2}·K^{-1}, $\eta_{EL,REF} = 0.1366$, $\gamma_{PVT} = 0.42$ %·K^{-1}, $T_{CELL,REF} = 56$ °C # of PV/Ts: 100, 200, 300 …, 800, 900, 1000
ETC	Area 3.018 m^2, $\eta_{OPT} = 0.835$, $k_{1,ETC} = 1.56$ W·m^{-2}·K^{-1}, $k_{2,ETC} = 0.0017$ W·m^{-2}·K^{-2} # of ETCs: 100, 200, 300 …, 800, 900, 1000
Heat storage	21 m^3, 43 m^3, 64 m^3, 86 m^3, 172 m^3 (equivalent to 6 h, 12 h, 18 h, 24 h and 48 h of operation)
Auxiliary boiler	Gas fired, $\eta_{TH} = 0.95$

Three different operating mode of the SAHP are considered:

- Operating mode 1: the low temperature heat produced by the PV/Ts is used as cold heat source in the heat pump evaporator. The high temperature heat produced by the heat pump and by ETCs is used in the pasteurization process.
- Operating mode 2: the mid temperature heat produced by the ETCs is used as cold heat source in the heat pump evaporator. The high temperature heat produced by the heat pump is used in the pasteurization process. PV/Ts do not provide any heat.
- Operating mode 3: the high temperature heat produced by ETCs is used in the pasteurization process. Neither the heat pump nor PV/Ts provide any heat.

It is worth specifying that in all the operating modes, any heat excess is stored in the heat storage or, conversely, the auxiliary boiler supplies the heat shortage. Regarding the power production, the PV/Ts produce power also in Operating mode 2 and 3. The power is used to drive the SAHP system (compressor and pumps) and the excess power is assumed to be completely used by the industrial process.

4. Results

The analysis of the SAHP is carried out for the city of Milan and for one year of operation. Two steps are considered in the analysis. In the first step several simulations are run to assess the influence of the number of PV/Ts, of the number of ETCs and of the heat storage size. In the second step an optimization process is carried out to identify the best system configuration both from the energetic point of view and from the economic point of view.

Fig. 3 shows the influence of yearly electrical energy surplus (left) and thermal energy supplied by the auxiliary boiler (right) as a function of the number of PV/Ts (x-axis) and ETCs (y-axis) for a storage volume equal to 86 m^3. Starting from the electrical energy, a strong influence of the number of PV/Ts and a weak influence of the number of ETCs are found. Indeed, for any size of the ETC field, the electrical energy surplus increases significantly as the number of PV/Ts increases whereas, for any size of the PV/T field, the electrical it is almost constant if the number of ETCs is higher than a threshold value, approximately 100-140. Below this value, an increase in the heat pump operating time arises which, in turn, lead to an increase in electricity consumption and, therefore, a reduction in the electrical energy surplus. Considering the thermal energy supplied by the auxiliary boiler, the opposite trend is found since a strong influence of the number of ECTs and a weak influence of the number of PV/Ts arise. Quite obviously, for any PV/T field size, the amount of heat the auxiliary boiler has to provide reduces as the number of ETCs increases whereas, for any size of the ETC field, this parameter is almost constant as a function of the number of PV/Ts. The only exception to this analysis is the bottom-left corner where the number of PV/Ts and ETCs is too low to drive the heat pump, resulting in a large use of the auxiliary boiler

to supply heat.

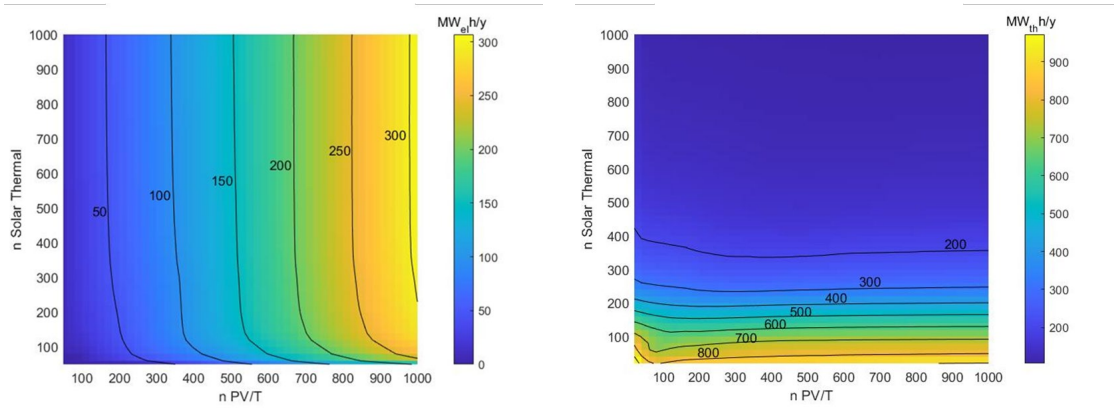

Fig. 3: Yearly electrical energy surplus (left) and thermal energy supplied by the auxiliary boiler (right) as a function of the number of PV/Ts (x-axis) and ETCs (y-axis) for a storage volume equal to 86 m^3.

The share of the heat production as a function of storage size (x-axis) and for some selected sizes of PV/T and ETC field (labels inside each bar) is reported in Fig. 4. First, a clear influence of the heat storage size may be found. Indeed, whatever is the number of PV/Ts or ETCs, the higher is the heat storage size, the lower is the auxiliary boiler share (green bars). Considering the production of process heat through ECTs (purple bars in operating mode 3 and red bar in operating mode 1), it is found that, with the only exception of the smaller storage size case, this operating mode achieves the highest share and, additionally, larger ETCs field (2nd and 4th purple bar in each group) benefit from the heat storage size more than smaller fields (1st and 3rd purple bar). The contribution of the SAHP to the share is largely dominated by the PV/T driven operating mode (operating mode 1, blue bars) rather than the ETC driven operating mode (operating mode 2, dark yellow bars) with an overall share of the SAHP almost constant and around 15%.

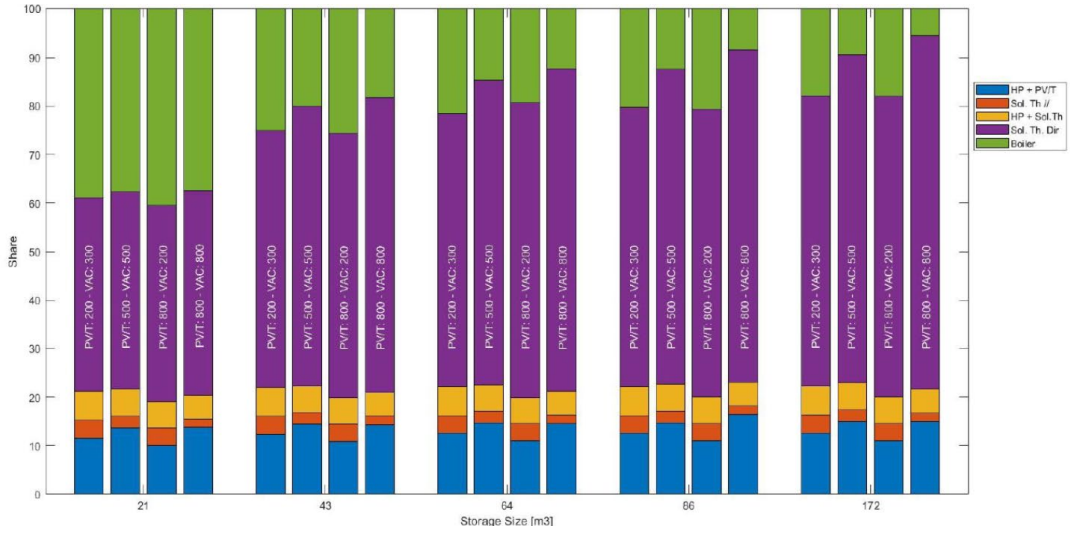

Fig. 4: Share of the heat production as a function of storage size

Once a general analysis of the overall performance is made, an energetic and economic optimization of the SAHP system is carried out. In the economic analysis, the cost of the auxiliary boiler is not considered since this component has to be used in any SAHP system. It is worth specifying that the energetic optimization is carried out with the aim of minimizing the auxiliary boiler consumption, whereas the economic optimization maximizes the Net Present Value (NPV) of the SAHP system. The cost of the components of the SAHP system are taken from a market survey and are collected in Tab. 2.

Tab. 2: Cost of the components of the SAHP system

Component	Cost
Heat pump	65270 €
PV/T	1200 €·(kW)$^{-1}$
ETC	850 €·m^{-2}
Heat storage	1500 €·m^{-3}

The results of the energetic or the economic optimization are reported in Tab. 3 and Tab. 4 respectively. As a first general comment it is possible to state that both the energetic and the economic optimal configurations lead to a reduction of the auxiliary boiler consumption since in the "boiler-only" scenario it accounts for 1158 MWh. Additionally, comparing the two sets of optimal configurations, it is found that the number of PV/Ts is equal to the maximum allowed by the problem constraints whereas the number of ETCs is 70%-150% higher in the optimal energetic configuration. Quite obviously, due to the larger ETC field size, the optimal energetic configuration has lower heat pump consumption, in the range 90.8% to 93.6% and, more importantly, significantly lower auxiliary boiler consumption, spanning the interval 49.1% to 83.8%. Conversely, the optimal economic configurations show superior economic parameters since the NPV is 26.9%-52.3% higher than the corresponding parameter in the optimal energetic configurations and, consequently, the pay-back time is 22.6%-39.8% lower. It is anyway quite interesting to state that the best optimal energetic configuration is achieved when the heat storage size is equal to 172 m^3, whereas in the best optimal economic configuration the storage size is equal to 43 m^3 considering the NPV and equal to 21 m^3 considering the IRR and the pay-back time.

Tab. 3: Optimal energetic configuration that minimizes the auxiliary boiler consumption

Storage size	21 m^3	43 m^3	64 m^3	86 m^3	172 m^3
Number of PV/Ts	1000	1000	1000	1000	1000
Number of ETCs	400	480	480	460	440
SAHP consumption	30.7 MWh	30.2 MWh	30.2 MWh	30.3 MWh	30.5 MWh
Auxiliary boiler consumption	455.1 MWh	245.2 MWh	181.1 MWh	158.9 MWh	129.2 MWh
NPV	673.2 k€	716.2 k€	756.7 k€	793.1 k€	739.6 k€
IRR	9.8%	9.4%	9.5%	9.7%	9.1%
PBT	12.8 y	13.4 y	13.2 y	12.8 y	13.7 y

Tab. 4: Optimal economic configuration that maximizes the NPV

Storage size	21 m^3	43 m^3	64 m^3	86 m^3	172 m^3
Number of PV/Ts	1000	1000	1000	1000	1000
Number of ETCs	160	220	240	240	260
SAHP consumption	33.8 MWh	32.8 MWh	32.7 MWh	32.7 MWh	32.6 MWh
Auxiliary boiler consumption	543.3 MWh	374.4 MWh	320.8 MWh	311.8 MWh	263.1 MWh
NPV	1025 k€	1083 k€	1071 k€	1050 k€	939 k€
IRR	15.7%	14.4%	13.6%	13.2%	11.4%
PBT	7.7 y	8.3 y	8.8 y	9.1 y	10.6 y

5. Conclusions

In the present study an energetic and economic analysis of a solar assisted heat pump system for pasteurization process is carried out.

First, the influence of the number of PV/Ts, the number of ETCs and the storage size on the system performance is analyze finding that the PV/T field size has a significant influence on the electric energy surplus and a negligible influence on the auxiliary boiler energy consumption, whereas the opposite occurs considering the size of the ETC field. Additionally, larger heat storages allow to better exploit the solar radiation since they tend to reduce the auxiliary boiler energy consumption.

Then, the optimal system configuration from the energetic or the economic point of view is identified finding that both systems lead to a reduction of the auxiliary boiler consumption. Additionally, the optimal energetic configurations exhibit larger size of the ETC fields and lower heat pump and auxiliary boiler energy consumptions whereas the optimal economic configurations have superior NPV and IRR and lower pay-back time.

6. List of symbols

$a_1 \dots a_{10}$	Manufacturer's coefficients in eq. 1
A	Area, m^2
$b_1 \dots b_{10}$	Manufacturer's coefficients in eq. 2
$c_1 \dots c_3$	Pressure drop coefficients in eq. 13
c_P	Isobaric heat capacity, $J \cdot kg^{-1} \cdot K^{-1}$
G	Solar irradiance, $W \cdot m^{-2}$
h	Enthalpy, $J \cdot kg^{-1}$
h_C	Convective heat transfer coefficient $W \cdot m^{-2} \cdot K^{-1}$
k	Thermal conductivity, $W \cdot m^{-1} \cdot K^{-1}$
$k_{1,ETC}$	Manufacturer's coefficient in eq. 12, $m^2 \cdot K \cdot W^{-1}$
$k_{2,ETC}$	Manufacturer's coefficient in eq. 12, $m^2 \cdot K^2 \cdot W^{-1}$
$k_{1,PVT}$	Manufacturer's coefficient in eq. 11, $m^2 \cdot K \cdot W^{-1}$
$\dot{m}$	Mass flow rate, $kg \cdot s^{-1}$
NTU	Number of transfer unit, dimensionless
$p_{O,GC}$	Refrigerant pressure at gas cooler outlet, kPa
$\dot{Q}$	Heat transfer rate, W
R^*	Heat capacity rates ratio, dimensionless
t	Thickness, m
T_E	Evaporating temperature, K
U	Overall heat transfer coefficient, $W \cdot K^{-1}$
$\dot{v}$	Volumetric flow rate, $m^3 \cdot s^{-1}$
$\dot{W}$	Power, W

Greek symbols

γ_{PVT}	Power coefficient in eq. 10

Δp	Pressure drop, Pa
ε	Effectiveness, dimensionless
η	Efficiency, dimensionless

Subscripts

A	Air
C	Cold stream
DIS	Compressor discharge
EL	Electrical
H	Hot stream
IN	Inlet
MAX	Maximum
OPT	Optical
OUT	Outlet
$PUMP$	Pump
REF	Reference condition
SUC	Compressor suction
TH	Thermal
W	Wall or water

7. References

Arpagaus, C., Bless, F., Uhlmann, M., Schiffmann, J., & Bertsch, S. S., 2018. High temperature heat pumps: Market overview, state of the art, research status, refrigerants, and application potentials. Energy 152, 985-1010, https://doi.org/10.1016/j.energy.2018.03.166.

Brückner, S., Liu, S., Miró, L., Radspieler, M., Cabeza, L.F., Lävemann, E. 2015. Industrial waste heat recovery technologies: An economic analysis of heat transformation technologies, Appl. Energ. 151, 157-167, http://dx.doi.org/10.1016/j.apenergy.2015.01.147.

Dabiri, A.E., Rice, C.K., 1981. A compressor simulation model with corrections for the level of suction gas superheat. ASHRAE Transactions 87 (Part 2), 771-782.

Eurostat, 2021. https://ec.europa.eu/eurostat/statistics-explained/index.php?title=Energy_statistics_-_an_overview#Final_energy_consumption. Last accessed 30/09/2021.

Kamel, R.S., Fung, A.S., Dash, P.R.H., 2015. Solar systems and their integration with heat pumps: A review. Energ. Buildings 87, 395-412, http://dx.doi.org/10.1016/j.enbuild.2014.11.030.

Lazzarin, R., 2020. Heat pumps and solar energy: A review with some insights in the future. Int. J. Refrig. 116, 146-160, https://doi.org/10.1016/j.ijrefrig.2020.03.031.

Lemmon, E., Huber, M., McLinden, M., 2013. NIST Standard Reference Database 23: Reference Fluid Thermodynamic and Transport Properties-REFPROP, Version 9.1. National Institute of Standards and Technology, Standard Reference Data Program, Gaithersburg.

Longo, G. A., Mancin, S., Righetti, G., Zilio, C., 2015. A new model for refrigerant boiling inside Brazed Plate Heat Exchangers (BPHEs). Int. J. Heat Mass Transf. 91, 144-149, http://dx.doi.org/10.1016/j.ijheatmasstransfer.2015.07.078.

Mohanraj, M., Belyayev, Ye., Jayaraj, S., Kaltayev, A., 2018. Research and developments on solar assisted compression heat pump systems – A comprehensive review (Part-B: Applications). Renew. Sust. Energ. Rev. 83, 124-155, http://dx.doi.org/10.1016/j.rser.2017.08.086.

Papapetrou, M., Kosmadakis, G., Cipollina, A., La Commare, U., Micale, G., 2018. Industrial waste heat: Estimation of the technically available resource in the EU per industrial sector, temperature level and country. Appl. Therm. Eng. 138, 207-216, https://doi.org/10.1016/j.applthermaleng.2018.04.043.

Simonetti, R., Molinaroli, L., Manzolini, G., 2019. Experimental and analytical study of an innovative integrated dual-source evaporator for solar-assisted heat pumps. Sol. Energy 194, 939-951, https://doi.org/10.1016/j.solener.2019.10.070.

Simonetti, R., Moretti, L., Molinaroli, L., Manzolini, G., 2020. Energetic and economic optimization of the yearly performance of three different solar assisted heat pump systems using a mixed integer linear programming algorithm. Energ. Convers. Manage. 206, paper 112446, https://doi.org/10.1016/j.enconman.2019.112446.

Zondag, H.A., de Vries, D.W., van Helden, W.G.J, van Zolingen, R.J.C., 2003. The yield of different combined PV-thermal collector designs. Sol. Energy 74, 253-269, doi:10.1016 / S0038-092X(03)00121-X.

Van de Bor, D. M., Infante Ferreira, C. A., 2013. Quick selection of industrial heat pump types including the impact of thermodynamic losses. Energy 53, 312-322, http://dx.doi.org/10.1016/j.energy.2013.02.065.